

Synthesis of a Chiral Crystal Form of MOF-5, CMOF-5, by Chiral Induction

Shi-Yuan Zhang,^{†,‡} Dan Li,[§] Dong Guo,[§] Hui Zhang,[§] Wei Shi,[‡] Peng Cheng,[‡] Lukasz Wojtas,^{||} and Michael J. Zaworotko^{*,†}

[†]Department of Chemical & Environmental Science, Materials and Surface Science Institute, University of Limerick, Limerick V94 T9PX, Republic of Ireland

[‡]Department of Chemistry, Key Laboratory of Advanced Energy Materials Chemistry (MOE), Collaborative Innovation Center of Chemical Science and Engineering, Nankai University, Tianjin 300071, P. R. China

[§]Department of Chemistry, College of Chemistry and Chemical Engineering, Xiamen University, Xiamen 361005, P. R. China

^{||}Department of Chemistry, University of South Florida, 4202 East Fowler Avenue, CHE205, Tampa, Florida 33620, United States

Supporting Information

ABSTRACT: Chiral variants of the prototypal metal–organic framework MOF-5, Λ -CMOF-5 and Δ -CMOF-5, have been synthesized by preparing MOF-5 in the presence of L-proline or D-proline, respectively. CMOF-5 crystallizes in chiral space group $P2_13$ instead of $Fm\bar{3}m$ as exhibited by MOF-5. The phase purity of CMOF-5 was validated by single-crystal and powder X-ray diffraction, infrared spectroscopy, thermogravimetric analysis, N_2 adsorption, microanalysis, and solid-state vibrational circular dichroism. CMOF-5 undergoes a reversible single crystal-to-single crystal phase change to MOF-5 when immersed in a variety of organic solvents, although *N*-methyl-2-pyrrolidone (NMP) does not induce loss of chirality. Indeed, MOF-5 undergoes chiral induction when immersed in NMP, affording racemic CMOF-5.

Chirality is an essential feature of life and plays a vital role in various chemical and biological processes. Chirality in crystalline materials manifests itself in applications such as enantioselective separation,^{1–4} asymmetric catalysis,^{1–6} and nonlinear optical behavior.⁷ Metal–organic materials (MOMs)^{8–10} can combine chirality and nanoscale porosity in a single material. Syntheses of chiral MOMs have thus far tended to focus upon two main approaches: use of homochiral molecular building blocks (MBBs)^{1,11–14} and spontaneous resolution of chiral nets comprised of achiral MBBs.^{11,15–17} Homochiral MOMs are most typically generated through the former approach, with homochiral MBBs covalently bonded to the MOM framework as linking or pendant ligands. Such MOMs can be synthesized from homochiral starting materials or through post-synthetic modification (PSM).^{18–21} PSM exploits porosity to attach chiral moieties at organic linkers or unsaturated metal centers. Homochiral MOMs produced by PSM tend to exhibit reduced or lost pore volume, but bulk chirality can also be created through MOMs that exhibit network topology that is inherently chiral because of the spatial organization of achiral building blocks. Unfortunately, such MOMs tend to form through spontaneous resolution, and they are typically racemic conglomerates (heterochiral).

An approach to synthesis of chiral MOMs that might overcome the drawbacks of the aforementioned methods is the use of chiral additives that induce achiral MBBs to generate homochiral MOMs. Such chiral induction remains poorly understood, but it offers the advantage that, in principle, it is not limited to particular MBBs or linkers. Recent examples of this approach include the syntheses of SIMOF-1 and $[Mn_3(HCOO)_4(adc)]$ by Morris²² and Bu,²³ respectively. Nevertheless, the use of chiral induction to crystallize chiral MOMs with a particular composition and topology remains under-studied, especially with respect to high-symmetry MBBs that crystallize in high-symmetry space groups.

In this Communication, we demonstrate that MOF-5,²⁴ a high-symmetry prototypal MOM that is one of the most widely studied metal–organic frameworks (MOFs),^{25–27} is subject to a phase change to a chiral variant during (chiral additives) or after (single crystal-to-single crystal transformation) synthesis. The existence of the new chiral variant of MOF-5, CMOF-5, is perhaps surprising given that MOF-5 is made from high-symmetry 6-connected tetranuclear Zn_4O clusters linked by 1,4-benzenedicarboxylate (BDC) linkers to form a primitive cubic or *pcu* network. Figures 1 and 2 illustrate how chiral additives (during synthesis) or solvent (post-synthesis) can induce the formation of CMOF-5.

Λ -CMOF-5 and Δ -CMOF-5 were synthesized from a 1:1:1 mixture of $Zn(NO_3)_2 \cdot 6H_2O$, H_2BDC , and L-proline or D-proline, respectively, in *N*-methyl-2-pyrrolidone (NMP) and water (4:1 v/v) at 120 °C. Single-crystal X-ray diffraction studies (detailed in SI and Table S1) conducted upon CMOF-5 revealed that it crystallizes in the chiral cubic space group $P2_13$ and that chirality results from a distortion of the backbone of the framework. A decrease in the unit cell parameter, 25.7726(10) Å in MOF-5 to 25.3688(7) Å in Λ -CMOF-5, is accompanied by a corresponding 4.63% decrease in the unit cell volume. The Zn–O bond distances within the Zn_4O MBBs are 1.9329(6) Å in MOF-5 and 1.909(17)–1.951(6) Å in Λ -CMOF-5. The lower symmetry of CMOF-5 is illustrated by the wave-like nature of its structure that results from twisting of

Received: October 25, 2015

Published: November 25, 2015

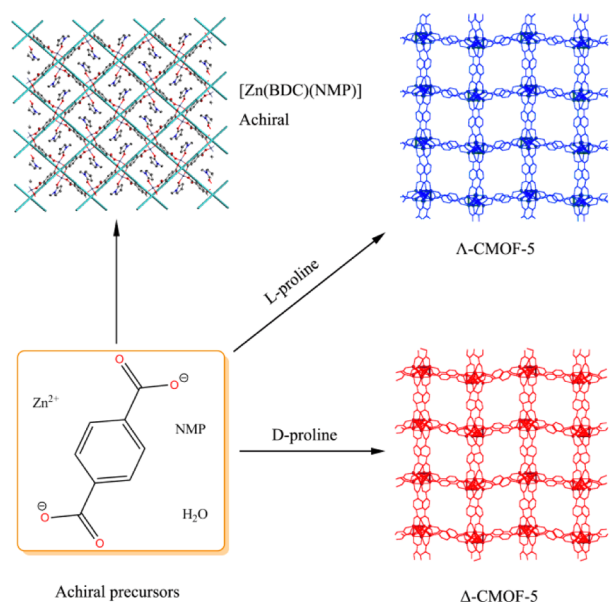


Figure 1. Synthesis of CMOF-5. The presence of *L*- or *D*-proline additives induces chirality and enables the growth and isolation of CMOF-5 crystals. An achiral square grid net, [Zn(BDC)(NMP)], forms in the absence of proline.

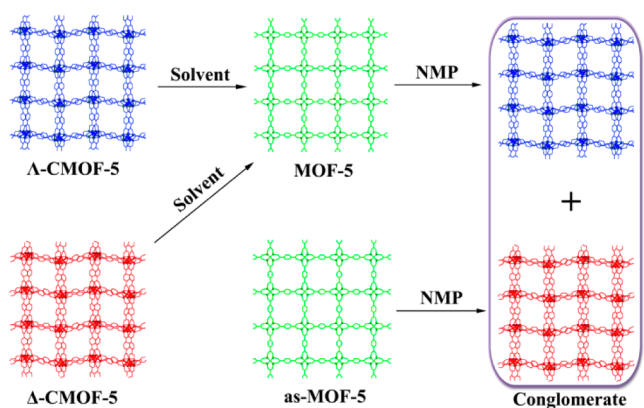


Figure 2. Post-synthetic modification studies conducted upon CMOF-5. PSM using most organic solvents converted CMOF-5 into MOF-5, whereas NMP induced MOF-5 to revert to a racemic conglomerate of CMOF-5.

adjacent Zn_4O clusters by 6.80° (Λ -CMOF-5) and 7.05° (Δ -CMOF-5) vs MOF-5 (Figures 3 and S1). The benzene rings between adjacent metal clusters in CMOF-5 are oriented at a non- 90° dihedral angle, giving rise to axial chirality. As a result of disordered BDC ligands, the torsion angles in Λ -CMOF-5 and Δ -CMOF-5, measured by taking the average of two disordered phenyl planes, are 78.68° and 66.85° , respectively. It appears that the atropisomer-like bridging mode of the ligands translates chirality from one cluster to another, thereby affording the observed chiral framework. To further understand the nature of chirality in CMOF-5, the building blocks are simplified as a single handedness helix (Figure 3), which self-assembles to construct the observed helical framework. Powder X-ray diffraction (PXRD) distinguishes between MOF-5 and CMOF-5 thanks to the lower symmetry of CMOF-5 (Figure S2).

To more fully characterize CMOF-5 and determine the nature of the guests that reside inside the void spaces, we

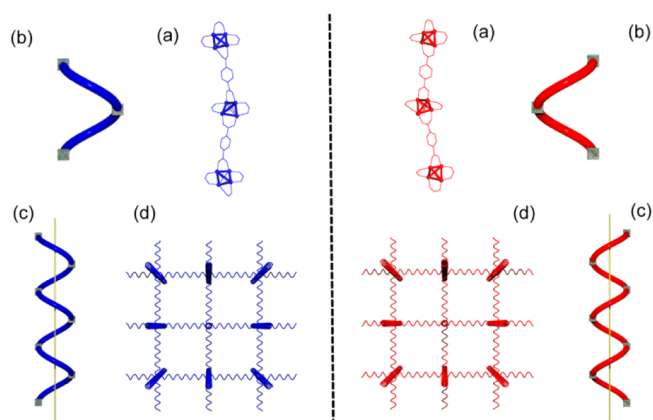


Figure 3. Formation of CMOF-5 structures: (a) Distorted metal clusters and BDC ligands. (b) A complete helix turn. Gray boxes represent Zn_4O clusters, and the BDC ligands generate the helical turns. (c) Assembly of helix fragments in one dimension. (d) Perspective view of CMOF-5. Color code: Λ -CMOF-5 in blue and Δ -CMOF-5 in red.

conducted IR spectroscopy, nitrogen gas adsorption, thermogravimetric analysis (TGA), and microanalysis experiments upon MOF-5 and CMOF-5 (see SI for details). IR spectroscopy (Figure S3) revealed the presence of the C=O stretching band of NMP at 1659 cm^{-1} and the absence the N–H bending band of proline at 1549 cm^{-1} , indicating that only NMP molecules are present in the channels of as-synthesized CMOF-5. IR spectroscopy was diagnostic with respect to CMOF-5 vs MOF-5 in that there are blue shifts of the C=O stretching band of BDC (1610 to 1598 cm^{-1}) and the O–Zn bending band of the Zn_4O cluster (1396 to 1378 cm^{-1}). Elemental analysis indicated that ~ 9.5 NMP per formula unit are incorporated in the channel, supported by the weight loss of 45.0% observed from TGA experiments (Figure S4). The nitrogen gas sorption isotherm (Figure S5) for activated CMOF-5 at 77 K exhibits type I behavior with a Langmuir surface area of $4535\text{ m}^2/\text{g}$, close to that reported for MOF-5.²⁸

The enantiomeric nature of Λ -CMOF-5 and Δ -CMOF-5 was verified through solid-state vibrational circular dichroism (VCD) spectra obtained from individual single crystals that had been converted to KBr pellets. Although single crystals were obtained from synthesis, enantiomers cannot be identified by appearance because their morphologies are indistinguishable. Figure 4 reveals that Λ -CMOF-5 and Δ -CMOF-5 exhibit different Cotton effects in the wavelength range 1800–1300 nm, supporting the formation of left-handed or right-handed enantiomers from reactions conducted in the presence of *L*-proline or *D*-proline, respectively. VCD measurements were conducted upon a random set of 10 crystals from each crystallization batch (Figures S6 and S7). Enantiomeric excess ($ee = 100 \times (\Lambda - \Delta)/(\Lambda + \Delta)$) of ca. 80% was observed for both Λ -MOF-5 and Δ -MOF-5.

Interestingly, when the same reaction was conducted in the absence of *L*-proline or *D*-proline, a new achiral layered square-grid compound, [Zn(BDC)(NMP)], was formed. This finding suggests that the presence of proline is critical for the crystallization of Λ -CMOF-5 or Δ -CMOF-5 under the particular conditions used.

The behavior of CMOF-5 with respect to PSM induced by solvent was next investigated. Guest-induced changes between solid forms are an intriguing and largely under-studied aspect of

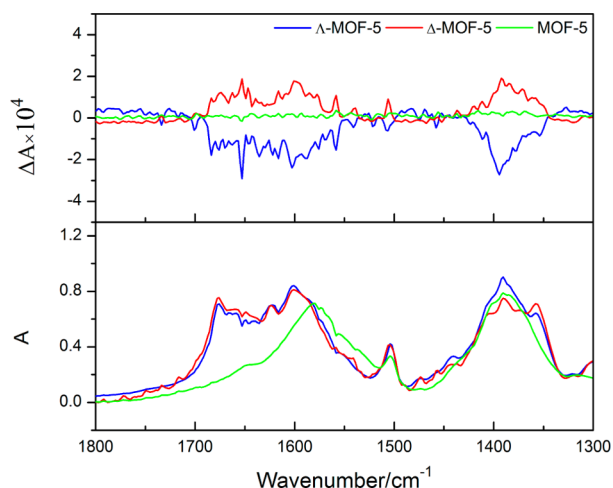


Figure 4. Solid-state VCD (top) and IR (bottom) spectra of a representative single crystal of Λ -CMOF-5 (blue), Δ -CMOF-5 (red), and MOF-5 (green).

MOM chemistry, although post-synthetic exchange of framework metals^{29–31} or/and ligands^{32–34} is becoming more widely studied. Direct observation of the location of guest molecules in void spaces would allow us to rationalize the effect of guest upon the coordination space around the MBBs, but this was not possible because of crystallographic disorder. Nevertheless, the overall effect of solvent exchange upon crystals of CMOF-5 immersed in a range of organic solvents could be readily evaluated. As revealed by Figure S8, in most instances CMOF-5 transformed to MOF-5, as evidenced by diagnostic calculated MOF-5 peaks. However, NMP, which presumably engages in strong interactions with the framework through hydrogen-bonding and/or C–H $\cdots\pi$ interactions, does not induce a phase change in CMOF-5. In order to further elucidate the role of NMP, as-synthesized MOF-5 and MOF-5 obtained indirectly from CMOF-5 were immersed in NMP, and phase transformation to CMOF-5 occurred within several hours. The outcomes of these phase transformations were validated by PXRD experiments (Figures 3 and S9) since there were no differences in morphology, color, or transparency. Solid-state VCD spectra of these crystals are presented in Figure S10 and indicate a racemic mixture of enantiomers. Therefore, although NMP is achiral, it is capable of chiral induction on MOF-5 but only to a racemic conglomerate.

In conclusion, we have demonstrated that MOF-5 can exist as a chiral variant, CMOF-5, that can be isolated through either of two simple methods: chiral induction using homochiral amino acid additives during synthesis, or, most surprisingly, PSM of MOF-5 into CMOF-5 induced by NMP, an achiral solvent. This behavior is somewhat related to the phenomenon of polymorphism,³⁵ but there is no direct analogy with phase changes in densely packed crystalline solids. Rather, the observed behavior appears to be an artifact of the nanoporous structure and chemical composition of MOMs. The discovery that molecules such as NMP can induce chirality in a high-symmetry MOM such as MOF-5 is an unexpected aspect of MOM chemistry that, if it proves to be general in nature, will provide a new avenue for both fundamental and applied studies of chirality in porous crystalline MOMs.

■ ASSOCIATED CONTENT

📄 Supporting Information

The Supporting Information is available free of charge on the ACS Publications website at DOI: 10.1021/jacs.5b11150.

- Information on materials and measurements; synthesis and characterization data; supplementary figures (PDF)
- X-ray crystallographic data for Δ -CMOF-5 (CIF)
- X-ray crystallographic data for Λ -CMOF-5 (CIF)
- X-ray crystallographic data for [Zn(BDC)(NMP)] (CIF)

■ AUTHOR INFORMATION

Corresponding Author

*xtal@ul.ie

Notes

The authors declare no competing financial interest.

■ ACKNOWLEDGMENTS

M.J.Z. acknowledges the U.S. Department of Energy (DE-AR000177) and Science Foundation of Ireland (Award 13/RP/B2549). W.S. and P.C. acknowledge the MOST (973 program, 2012CB821702), NSFC (21373115, 21331003, and 91422302), and 111 Project (B12015).

■ REFERENCES

- (1) Seo, J. S.; Whang, D.; Lee, H.; Jun, S. I.; Oh, J.; Jeon, Y. J.; Kim, K. *Nature* **2000**, *404*, 982.
- (2) Nuzhdin, A.; Dybtsev, D.; Bryliakov, K.; Talsi, E.; Fedin, V. *J. Am. Chem. Soc.* **2007**, *129*, 12958.
- (3) Liu, Y.; Xuan, W.; Cui, Y. *Adv. Mater.* **2010**, *22*, 4112.
- (4) Kim, K.; Banerjee, M.; Yoon, M.; Das, S. *Top. Curr. Chem.* **2009**, *293*, 115.
- (5) Lee, J.; Farha, O. K.; Roberts, J.; Scheidt, K. A.; Nguyen, S. T.; Hupp, J. T. *Chem. Soc. Rev.* **2009**, *38*, 1450.
- (6) Yoon, M.; Srirambalaji, R.; Kim, K. *Chem. Rev.* **2012**, *112*, 1196.
- (7) Long, N. J. *Angew. Chem., Int. Ed. Engl.* **1995**, *34*, 21.
- (8) Perry, J. J., IV; Perman, J. A.; Zaworotko, M. J. *Chem. Soc. Rev.* **2009**, *38*, 1400.
- (9) Batten, S. R.; Neville, S. M.; Turner, D. R. *Coordination Polymers: Design, Analysis and Application*; Royal Society of Chemistry: Cambridge, UK, 2009.
- (10) MacGillivray, L. R. *Metal–Organic Frameworks: Design and Application*; John Wiley & Sons: Hoboken, NJ, 2010.
- (11) Morris, R.; Bu, X. *Nat. Chem.* **2010**, *2*, 353.
- (12) Zhang, S.-Y.; Wojtas, L.; Zaworotko, M. J. *J. Am. Chem. Soc.* **2015**, *137*, 12045.
- (13) Anokhina, E.; Go, Y.; Lee, Y.; Vogt, T.; Jacobson, A. *J. Am. Chem. Soc.* **2006**, *128*, 9957.
- (14) Ma, L.; Abney, C.; Lin, W. *Chem. Soc. Rev.* **2009**, *38*, 1248.
- (15) Pérez-García, L.; Amabilino, D. *Chem. Soc. Rev.* **2002**, *31*, 342.
- (16) Kepert, C. J.; Prior, T. J.; Rosseinsky, M. J. *J. Am. Chem. Soc.* **2000**, *122*, 5158.
- (17) Biradha, K.; Seward, C.; Zaworotko, M. J. *Angew. Chem., Int. Ed.* **1999**, *38*, 492.
- (18) Wu, C.-D.; Lin, W. *Angew. Chem., Int. Ed.* **2005**, *44*, 1958.
- (19) Banerjee, M.; Das, S.; Yoon, M.; Choi, H. J.; Hyun, M. H.; Park, S. M.; Seo, G.; Kim, K. *J. Am. Chem. Soc.* **2009**, *131*, 7524.
- (20) Lun, D. J.; Waterhouse, G. I. N.; Telfer, S. G. *J. Am. Chem. Soc.* **2011**, *133*, 5806.
- (21) Wang, Z.; Cohen, S. M. *Chem. Soc. Rev.* **2009**, *38*, 1315.
- (22) Lin, Z.; Slawin, A.; Morris, R. *J. Am. Chem. Soc.* **2007**, *129*, 4880.
- (23) Zhang, J.; Chen, S.; Nieto, R.; Wu, T.; Feng, P.; Bu, X. *Angew. Chem., Int. Ed.* **2010**, *49*, 1267.
- (24) Li, H.; Eddaoudi, M.; O’Keeffe, M.; Yaghi, O. M. *Nature* **1999**, *402*, 276.

- (25) Eddaoudi, M.; Kim, J.; Rosi, N.; Vodak, D.; Wachter, J.; O’Keeffe, M.; Yaghi, O. M. *Science* **2002**, *295*, 469.
- (26) Long, J. R.; Yaghi, O. M. *Chem. Soc. Rev.* **2009**, *38*, 1213.
- (27) Zhou, H.-C.; Long, J. R.; Yaghi, O. M. *Chem. Rev.* **2012**, *112*, 673.
- (28) Kaye, S. S.; Dailly, A.; Yaghi, O. M.; Long, J. R. *J. Am. Chem. Soc.* **2007**, *129*, 14176.
- (29) Das, S.; Kim, H.; Kim, K. *J. Am. Chem. Soc.* **2009**, *131*, 3814.
- (30) Kim, M.; Cahill, J. F.; Fei, H.; Prather, K. A.; Cohen, S. M. *J. Am. Chem. Soc.* **2012**, *134*, 18082.
- (31) Lalonde, M.; Bury, W.; Karagiari, O.; Brown, Z.; Hupp, J. T.; Farha, O. K. *J. Mater. Chem. A* **2013**, *1*, 5453.
- (32) Karagiari, O.; Bury, W.; Mondloch, J. E.; Hupp, J. T.; Farha, O. K. *Angew. Chem., Int. Ed.* **2014**, *53*, 4530.
- (33) Deria, P.; Mondloch, J. E.; Karagiari, O.; Bury, W.; Hupp, J. T.; Farha, O. K. *Chem. Soc. Rev.* **2014**, *43*, 5896.
- (34) Li, T.; Kozlowski, M.; Doud, E.; Blakely, M.; Rosi, N. *J. Am. Chem. Soc.* **2013**, *135*, 11688.
- (35) Bernstein, J. *Cryst. Growth Des.* **2011**, *11*, 632.